SCAL model for CCS – Insights from the first commercial CO_2 project on the Norwegian Continental Shelf, Northern Lights

Einar Ebeltoft[1)], Marion Recordon[2)], Renata Meneguolo[2), 3)] Jørgen Gausdal Jacobsen[1), 3)], Reza Askarinezhad[4)], and Richy Pitman[2)]*

[1)] Equinor ASA, Bergen, Norway, [2)] Equinor ASA, Stavanger, Norway, [3)] NL DA, Stavanger, Norway, [4)] NORCE, Stavanger Norway

Abstract. Relative permeability and capillary pressure are multi-phase flow properties characterized by a SCAL-model that determine the reservoir fluid dynamics for the fields in production and for the new field developments. For Carbon Capture and Storage projects (CCS), multi-phase flow properties are equally important. Interpretation of SCAL experiments and implementation of the SCAL-model for full-field simulations will be shared to highlight the impact of the SCAL model uncertainty on the estimation of the carbon dioxide (CO_2) storage resource assessment and plume migration for the Northern Lights project - the world's first open-source CO_2 transport and storage infrastructure.

In case of CO_2 storage in the saline aquifer like in the Northern Lights project, the flow process is inverse to the hydrocarbons production as water saturation decreases from unity saturation toward a residual water saturation when the CO_2-plume propagates though the formation. Therefore, there is a need to provide the SCAL-model for the process and system applicable for CCS, i.e., primary drainage type when the CO_2 plume develops and residual trapped CO_2 when the aquifer later imbibes into the stored CO_2.

Nitrogen (N_2) has frequently been used by the industry at ambient conditions as proper analogue fluid to CO_2 to achieve fluid flow properties without the need for SCAL experiments at the resource-demanding reservoir conditions with supercritical CO_2. For the SCAL-model presented her, we have also included experiments with supercritical CO_2 at reservoir conditions. Several multi-phase flow experiments have been performed, and comprehensive interpretation work has been performed using the core flow simulations tool Sendra. The experiments cover steady state for relative permeabilities, multi speed centrifuge and porous plate for capillary pressure and residual water saturation, as well as unsteady state trapped gas experiments to provide data for determination of residual trapped CO_2.

1 Introduction

Over the past decades, and especially the recent years there has been an increased interest in Carbon Capture and Storage (CCS) by the industry in general and by the oil industry, especially. CCS has the potential to be an important technology toward the energy transition required for the next decades. The dynamic two-phase flow behaviour for CO_2 injection into an aquifer is similar to the traditional two-phase flow processes in an oil- or gas field.

The storage concept of the Northern Lights transport and geological sequestration project is of a gently (1-2 deg.) northwards sloping saline aquifer in the first CO_2 exploitation permit in Norway (EL001, Aurora), located south of the Troll field in the Horda Platform as shown in Fig. 1.

The storage complex in EL001 is composed by the Upper Triassic and Lower Jurassic Statfjord and Dunlin Group, with the Johansen Formation sandstone as injection target and the overlying Cook Formation as storage unit while the underlying sandstones of the Statfjord Group (Nansen and Eiriksson formations) are considered as an upside. Ultimately, migration would lead the CO_2 beneath the Troll West megaclosure, where structural trapping would increase storage security. The cap rock is the Drake Formation, also of Early Jurassic age, Fig. 2.

The Statfjord and Dunlin Groups record the transition from continental to marginal and shallow-marine setting and are considered favourable units for CO_2 sequestration because of lateral extent, connectivity, and reservoir properties and architecture, see [1] and references therein.

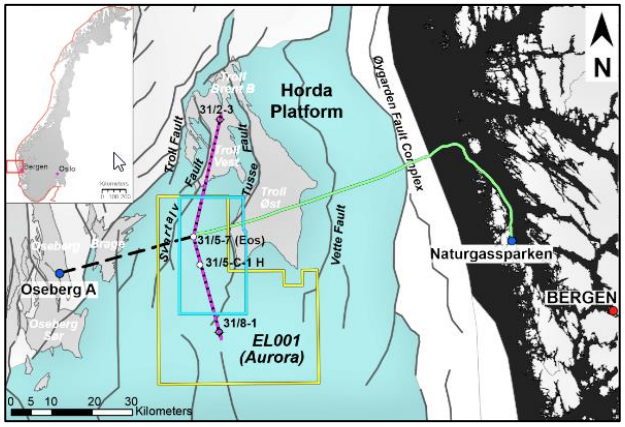

Fig. 1. Location of the Aurora storage site. Map of the main offshore features of the Northern Lights project: exploitation license EL001 (yellow polygon); pipeline from land (green line), umbilical (black, dashed line); trace of cross-section in 1B (pink dashed line).

* Corresponding author: eieb@equinor.com

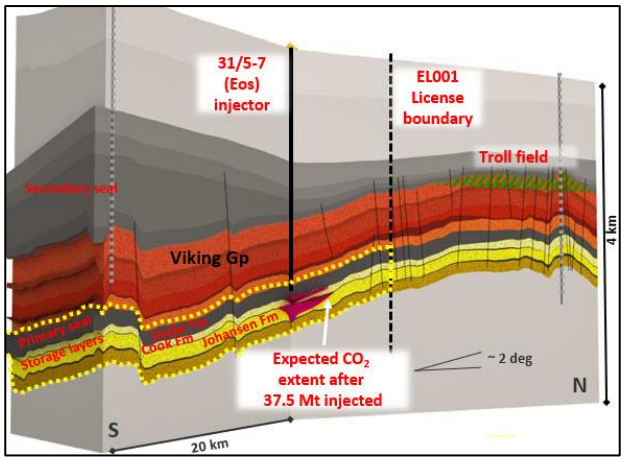

Fig. 2. Schematic cross section of the Storage Complex and expected plume development after 37,5 Mt injected. Trace in 1A (pink dashed line). Courtesy: Equinor, from seismic data from CGG.

No SCAL information for CCS was available from the Dunlin Group before the analyses carried out by Equinor on behalf of the EL001 operator Northern Lights JV. This paper bridges the gap between the static reservoir characterization and the dynamic behaviour.

The present focus for Northern Lights is the plume migration (primary drainage), while the long-term trapping mechanism (imbibition) due to buoyancy forces is of secondary order, presently. Apart from permeability of the formation, the dynamic of the plume migration is mainly characterised by the relative permeability curves, while the influence of capillary pressure will reduce the ultimate movement of the plume.

2 SCAL program

The SCAL-model presented in this paper is based upon a SCAL-program that includes several plugs checked for homogeneity by CT-scans from the main formations, Johansen and Cook. The permeability ranges are 50-100 md, 100-500 md and 500-3000 md, while porosity ranges from 20-30%. The SCAL sampling selection served two different purposes: provide measurements of the most volumetrically representative lithology [1], and to define the properties range for both injection and storage units. 42 plugs have been used for all together 52 experiments where some of the plugs have been re-used. The flow experiments were performed at both ambient and reservoir conditions, while the centrifuge and porous plate experiments were performed at ambient conditions due to present experimental limitations for both temperature and pore pressure. The number of experiments at ambient conditions and reservoir conditions are:

Relative permeability

- 6 Steady state, amb. cond, drainage
- 9 Single speed centrifuge, amb. cond, drainage
- 6 Unsteady state, trapped gas, amb. cond. imb.
- 5 Steady state, res. cond., drainage (2 ongoing)
- 6 Unsteady state, trapped gas, res.cond., imb.

Capillary pressure

- 9 Multi speed centrifuge, amb. cond, drainage
- 10 Porous plate, amb. cond, drainage

The steady state and unsteady state experiments utilized a composite core of two plugs, while the remaining experiments utilized single plugs. A selection of these individual experiments will be presented in the next section, while section 4 comprises all experiments to define a proper SCAL-model for Northern Lights.

The *steady state* experiments were performed from unity fractional flow of water to unity fractional flow of the gaseous phase, including rate bumps. The unsteady state experiments were performed with low-rate water injection and rate bumps, toward the trapped gaseous saturation. The *multi speed centrifuge* experiments were initiated at low rotational speed by increasing in steps to a maximum speed ensuring not to exceed the widely accepted Bond no. of 10^{-3} [2,3]. Similarly, *single speed experiments* were done by respecting the maximum Bond no. *Porous plate* experiments were also performed for the primary drainage process. The *unsteady state* imbibition experiments were initiated from residual water saturation, S_{wr}, established by either the centrifuge- or the porous plate technique.

The flow experiments monitor the progress of the time dependent properties: *differential pressure* across the composite core, *production* from the composite core and *in-situ water saturation measurement* (ISSM) along the composite core. The centrifuge- and porous plate experiments monitor the *production vs. time* from the plugs. Combining the information from both flow experiments and centrifuge/porous plate experiments provides consistent sets of relative permeability curves corrected for capillary end-effects with reliable saturation end points for residual water saturation, S_{wr}, and trapped gaseous saturation, S_{gt}.

2.1 Experiments, preparation and conditions

All plugs were drilled with water-based mud and cleaned by flooding synthetic formation water for around 10 PV, then followed by methanol to remove salt until negative $AgNO_3$ tests on effluent. Drying was performed by flooding N_2 through the core before helium pore volume and Klinkenberg corrected permeability were measured at ambient temperature and net confining pressure. The plugs were then saturated with synthetic formation water before measuring the absolute water permeability. Experimental conditions and fluid properties are given in Table 1 to Table 3.

Table 1: Experimental conditions.

Experimental condition	Temp. [°C]	Pore pressure [bar]	Net confining pressure [bar]
Ambient centrifuge	22	atm.	158
Ambient flow	35	20	158
Ambient porous plate	22	atm.	158
Reservoir flow	107	270	158

Table 2: Fluid properties, ambient conditions.

Temp. [ºC]	Visc. water [cP]	Density water [cc/g]	Visc. N_2 [cP]	Density N_2 [g/ml]
22	1.020	1.050	0.011	0.018
35	0.835	1.047	0.019	0.023

Table 3: Fluid properties, reservoir conditions.

Temp. [ºC]	Visc. water [cP]	Density water [cc/g]	Visc. CO_2 [cP]	Density CO_2 [g/ml]
107	0.296	1.038	0.047	0.594

3 SCAL-experiments: Results and interpretation

All experiments were interpreted by utilizing Sendra [4] for both curve-fitting the analytical data and history matching the experimental data by core flow simulations, see the section *Discussion* for further elaboration. The sequence of the interpretation was first to consider the multi speed centrifuge experiments to provide a reliable capillary pressure curve, residual water saturation, S_{wr}, and the gaseous end point relative permeability at residual water, $k_{rg}(S_{wr})$. Further the steady state two-phase flow experiments were reconciled by including the capillary pressure for the sister plug and anchoring the relative permeability curves in the end point determined by the multi speed centrifuge experiment. The purpose is to reconcile both types of experiments with similar set of relative permeability and capillary pressure curves [5]. The LET correlations for both relative permeability and capillary pressure [6,7] have been utilized.

To demonstrate the interpretation, we will show two sets of primary drainage experiments with interpretations, one at ambient conditions (synthetic formation water/N_2) and the other at reservoir conditions (synthetic formation water/scCO_2) – utilizing one multi speed centrifuge experiment and one steady state experiment. All experiments are interpreted similarly and used as input to the SCAL-model defined in section 4.

3.2.1 Ambient conditions

The experimental and simulated production data for the multi speed centrifuge capillary pressures experiment are shown in Fig. 3. The experimental production data is well reconciled by Sendra simulations, and the LET capillary pressure curve is shown in Fig. 4. The LET capillary pressure curve shows slight deviation from the Forbes analytical interpretation [8], and is regarded as reliable as the experimental data is well reconciled and the analytical interpretation can be subjected to error in water saturation up to 5-10% [9]. The last production steps of a multi speed centrifuge contains information of the displaced phase relative permeability curve, here k_{rw} toward S_{wr} – like single speed centrifuge experiments [10, 11]. The single speed centrifuge experiments in the SCAL program were not taken into account due to unreliable high residual water saturation, further outlined in section 6.

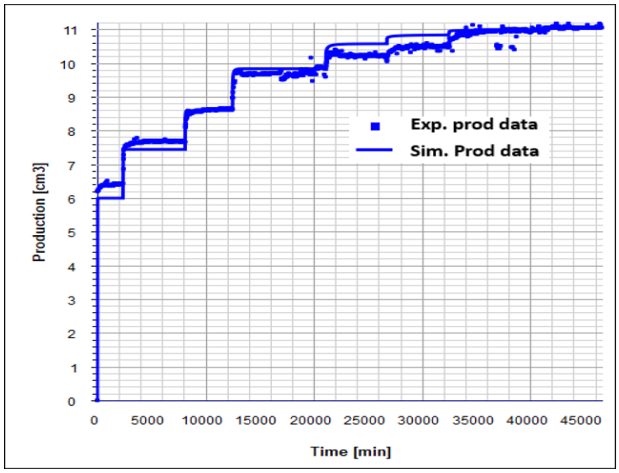

Fig. 3. Experimental and simulated production (history match) of the multi speed centrifuge experiment.

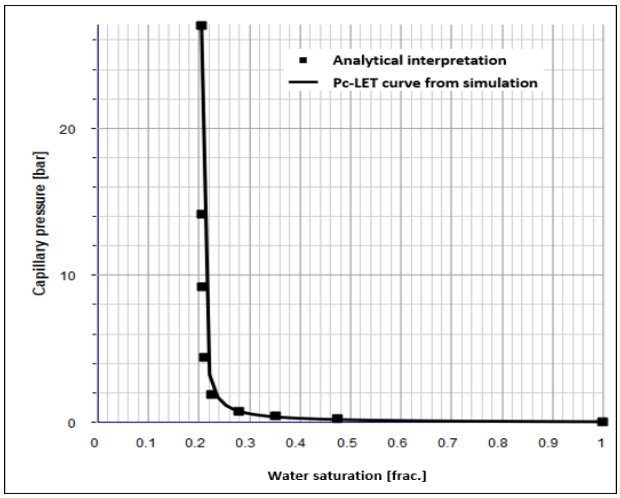

Fig. 4. LET capillary pressure determined by simulation (history match) shown together with analytical data.

For the steady state experiment, the experimental and simulated differential pressure and production data are shown in Fig. 5 while Fig. 6 shows the experimental and simulated water saturation profile along the composite core. These data are history matched by varying the relative permeabilities until the data are reconciled. The resulting relative permeability curves are shown in Fig. 7 and Fig. 8. The experimental data is well reconciled by these relative permeabilities, and the independently determined capillary pressure curve shown in Fig. 4.

These experiments are primary drainage experiments in strongly water-wet plugs where the capillary forces are significant. The viscous forces are not sufficient to overcome the capillary forces and we cannot expect to achieve even close to residual water saturation as illustrated by the saturation profiles in Fig. 6. Hence, it is a challenge to ensure reliable relative permeability curves for low water saturations. To compensate for this, we have used residual water saturation and information of the tail end water relative permeability from the multi speed centrifuge experiment.

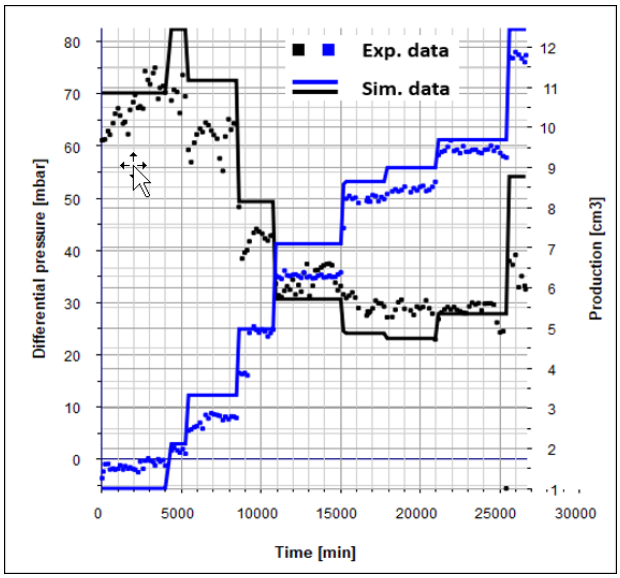

Fig. 5. Experimental and simulated differential pressure and production (history match) of the steady state experiment, at ambient coditions.

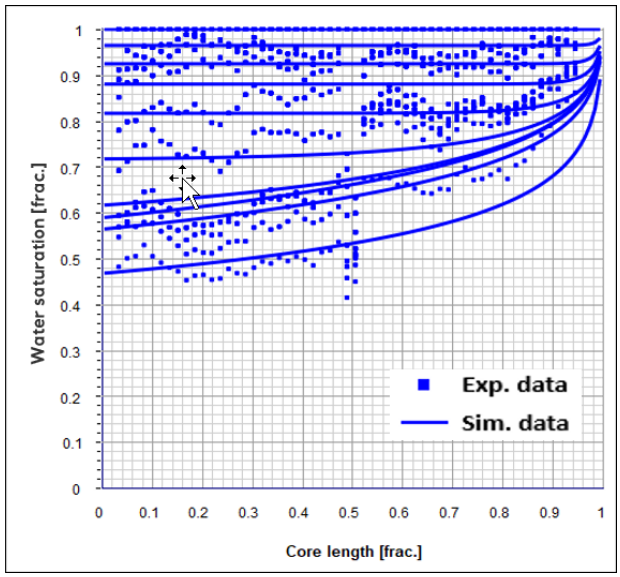

Fig. 6. Experimental and simulated water saturation profiles (history match) of the steady state experiment, at ambient conditions.

The expected depressed water relative permeability due to capillary forces are also observed in Fig. 8 by the circles where the analytical data deviate from the capillary pressure corrected water relative permeability curve at the end of production.

Another parameter to establish is the gaseous permeability at residual water, $k_{rg}(S_{wr})$. This property is not obtained by the steady state experiment but has been determined subsequent to the multi speed centrifuge and the porous plate experiments due to more realistic value of S_{wr}. The overall observation is that all $k_{rg}(S_{wr})$ in the SCAL program are in the region of unity when normalized to water relative permeability at unity water saturation. We have hence anchored all the gaseous relative permeability curves to unity.

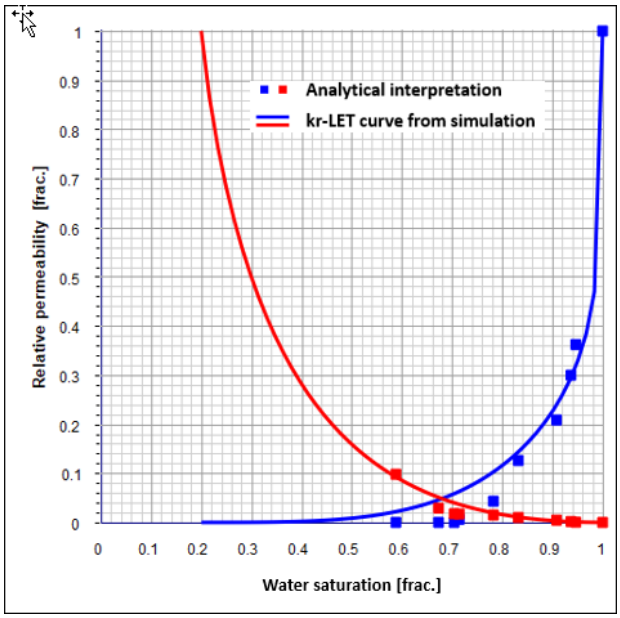

Fig. 7. LET relative permeability determined by simulation (history match) shown together with analytical data. Ambient conditions, lin-lin plot.

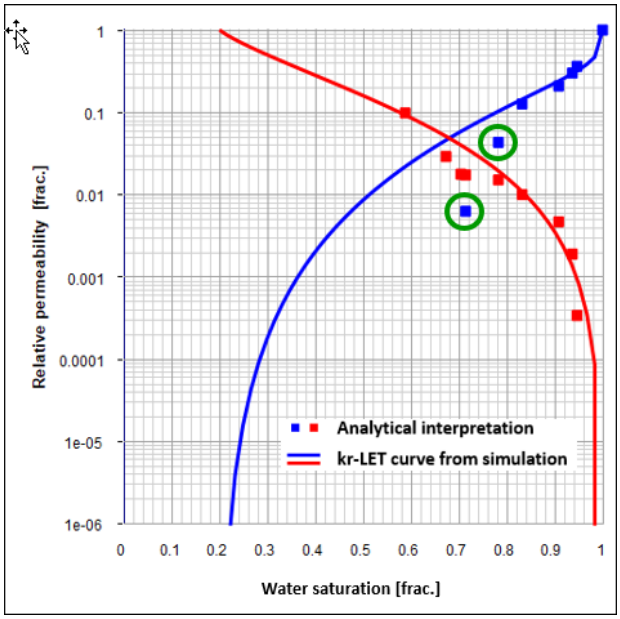

Fig. 8. LET relative permeability determined by simulation (history match) shown together with analytical data. Ambient conditions, semilog plot.

3.2.2 Reservoir conditions

The analysis and interpretation of the reservoir conditions steady state experiments are done similarly to the ambient condition described in the previous section. The experimental and simulated differential pressure and production data are shown in Fig. 9 while Fig. 10 shows the experimental and simulated water saturation profile along the plug at various time steps reflecting the decreasing injection of fractional flow of water. These experimental data are well reconciled by simulations.

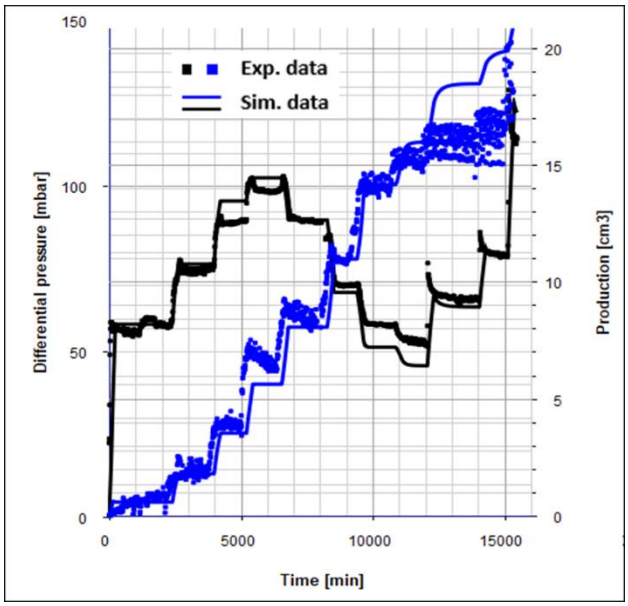

Fig. 9. Experimental and simulated differential pressure and production (history match) of the steady state experiment, at reservoir conditions.

The water saturation profiles in Fig. 10 shows ceasing production at around S_w=0.5 which is expected due to a primary drainage flow process influenced by capillary forces. Like the ambient condition experiment with N_2, the capillary end-effect is experienced as the viscous forces are not sufficient to overcome the capillary forces. For the reservoir condition experiment, we have used residual water saturation and information of the tail end water relative permeability from the ambient condition multi speed centrifuge.

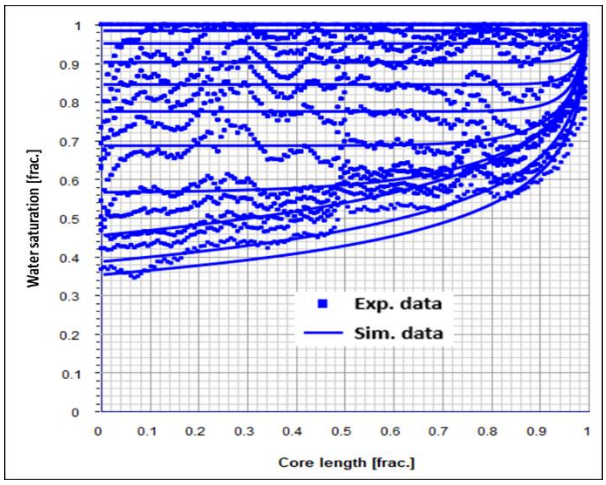

Fig. 10. Experimental and simulated water saturation profiles (history match) of the steady state experiment, at reservoir conditions.

The interpreted LET relative permeability curves are shown in Fig. 11 and Fig. 12. The curves interpreted by simulation and history matching the experimental data follows initially the analytical data but deviates toward the end of the steady state experiment. The analytical water relative permeability is depressed, similarly to the ambient condition experiments (Fig. 8). CO_2 relative permeability interpreted by simulations also deviates from the analytical relative permeabilities but provides a smooth curve that reconciles the experimental data. Relative permeability toward residual water saturation is presently supported by data obtained at ambient condition. The CO_2 relative permeability curve is fixed at unity for residual water saturation. This may change when further data is obtained in this saturation region at reservoir- or supercritical conditions [13].

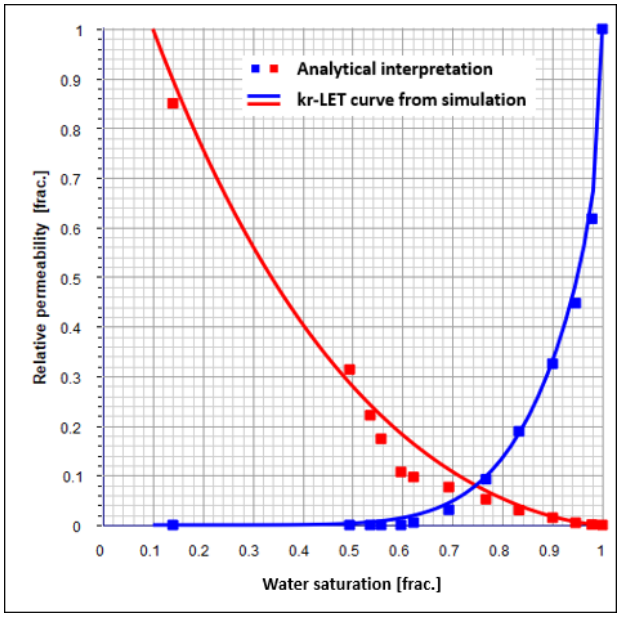

Fig. 11. LET relative permeability determined by simulation (history match) shown together with analytical data. Reservoir conditions, lin-lin plot.

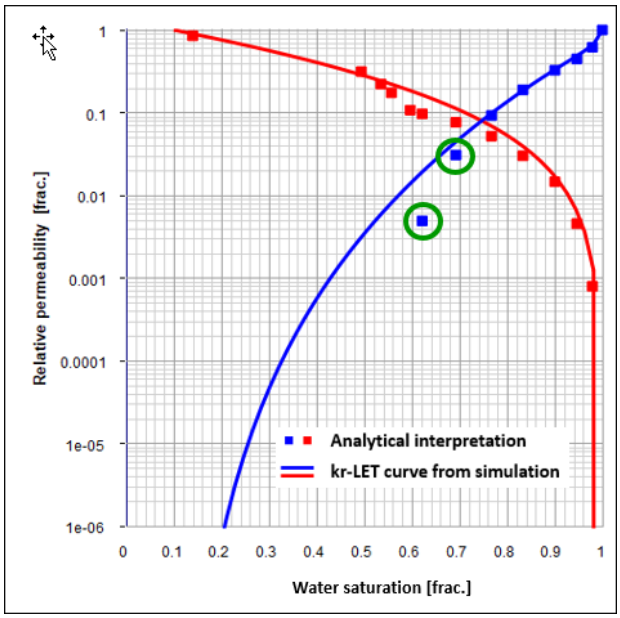

Fig. 12. LET relative permeability determined by simulation (history match) shown together with analytical data. Reservoir conditions, semilog plot.

The capillary pressure used when reconciling the experimental data in Fig. 9 and Fig. 10 differs from the one interpreted for the multi speed experiment, see Fig. 13. The capillary pressure applied in the steady state history match at reservoir conditions is lower than the capillary pressure obtained at ambient conditions, even though it is Leverett J-scaled by the interfacial tension

(IFT) and permeability. A default value for IFT for the formation water and N_2 at ambient condition of 72 mN/m has been used while IFT for formation water and CO_2 at reservoir conditions is in the vicinity of 30 mN/m [14].

This leads to the present hypothesis that the capillary pressure acting between water and CO_2 at reservoir- or supercritical condition is not similar to the capillary pressure obtained at ambient condition using N_2.

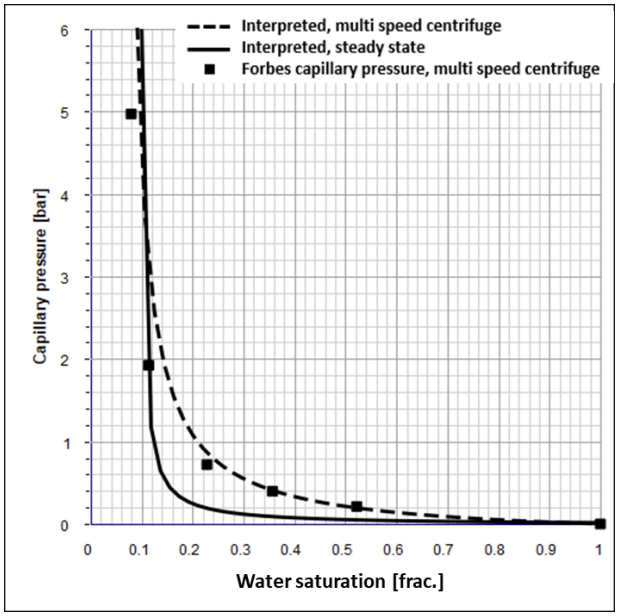

Fig. 13. Analytical and LET capillary pressure from multi speed centrifuge and LET capillary pressure used in the steady state simulation (history match).

4 SCAL-model and implementation

A SCAL-model for field application, commonly consists of a base case relative permeability curve with an uncertainty span, as an optimistic and a pessimistic case for comprising the uncertainties [15]. A comprehensive SCAL-model for CCS will contain the following flow properties and correlations:

- Primary drainage
  - Relative permeability
  - Capillary pressure
- Imbibition
  - Relative permeability, trapped CO_2
  - Utilize Land [16] and Killough [17]
- Correlation:
  - Residual water saturation vs. water permeability, S_{wr} vs. k_w
  - Trapped gas vs. initial water saturation, S_{gt} vs. S_{wi}

One common SCAL-model was established for Northern Lights as there is no obvious and significant correlation of the *shape* of the obtained relative permeabilities for the various permeability, porosity and formations. The SCAL-model is further scaled between zero and unity water saturation.

When the SCAL-model is utilised for full-field application, it should be re-scaled to acknowledge the dependency of residual water and the permeability, i.e., S_{wr} vs. k_w, in each grid cell in the dynamic reservoir model. Similarly, the trapped CO_2 should also acknowledge the well accepted dependency of initial gaseous saturation by the Land correlation [16].

The saturation end point correlations are established prior to defining the SCAL-model for primary drainage and imbibition.

4.1 S_{wr} vs. k_w correlation

Linear trends in semilog plots between residual water saturation, S_{wr}, and permeability, k_w, are established as shown for the Cook formation in Fig. 14 and for the Johansen formation in Fig. 15. Data utilized for these trends are all available in the present SCAL-program and comprises P_cH_g data, multi speed centrifuge- and porous plate data. The P_cH_g data is converted to CO_2/water system utilizing the Swanson permeability correlation [18].

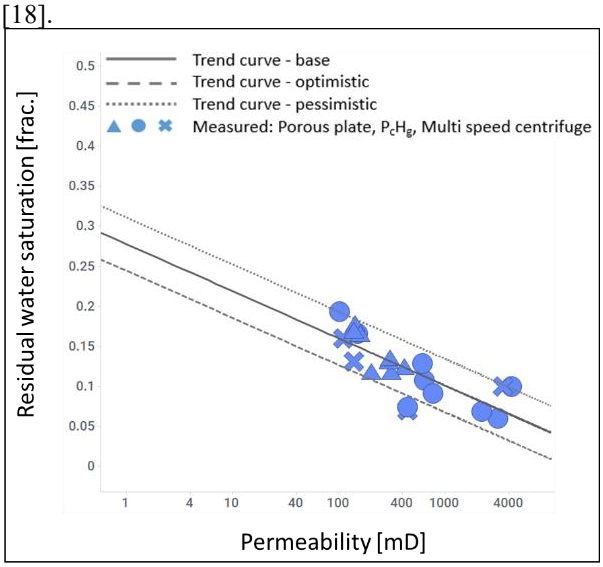

Fig. 14. Residual water saturation, S_{wr}, vs. permeability for the Cook formation.

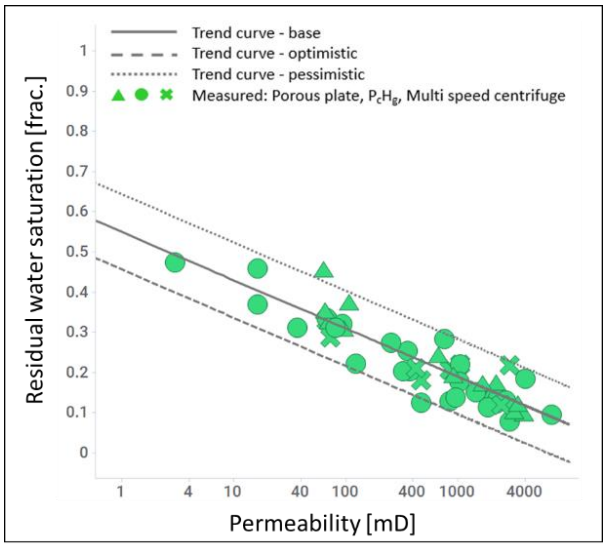

Fig. 15. Residual water saturation, S_{wr}, vs. permeability for the Johansen formation.

There are individual trends for the two formations – hence different correlations have been applied. Reason for the different trends is believed to be dual porosity for the

Johansen formation that was not observed for the Cook formation. The low trend curve for these correlations is regarded as optimistic, both with respect to plume migration as well as the storage capacity. The high trend is consequently regarded as pessimistic.

4.2 Trapped gas vs. initial saturation correlation

For long-term storage purposes, the buoyancy forces cause the aquifer to imbibe into the gaseous phase, i.e., CO_2, through an imbibition process and the CO_2 will be trapped. It is well accepted that the residual gaseous saturation depends upon initial water saturation and is commonly modelled by the Land correlation [16]. Trapped CO_2 will hence depend upon the residual water saturation determined through the correlations in Fig. 14 and Fig. 15 for the individual cells in the dynamic reservoir model.

The determined trapped gas saturations are shown in Fig. 16 together with values used for the Land correlation C-coefficient [16] and appropriate uncertainties.

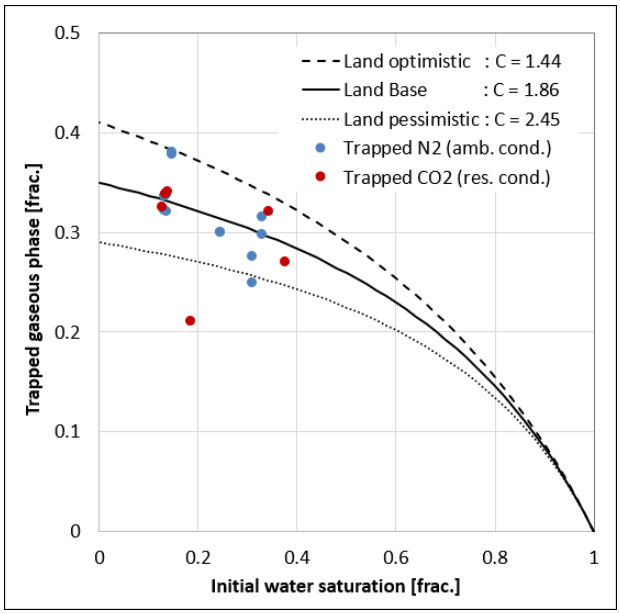

Fig. 16. Trapped gaseous phase (N_2 and CO_2) vs. initial water saturation with applied Land correlations.

4.3 Primary drainage, relative permeability and capillary pressure

The individual drainage steady state relative permeability curves obtained at ambient- and reservoir conditions are shown in Fig. 17 and Fig. 18, linlin- and semilog plot, respectively.

The end point CO_2 relative permeabilities, $k_{rCO2}(S_{wr})$, are based upon the N_2 relative permeability at residual water. All these measurements were in the region of unity, hence the gaseous relative permeabilities are anchored in unity. Apart from one of the ambient conditions N_2 relative permeability curves, all ambient conditions N_2 relative permeabilities are on or above the reservoir conditions CO_2 relative permeabilities. Reservoir condition water relative permeability for CO_2 does not drop as dramatic as the ambient conditions N_2 water relative permeability for high water saturation.

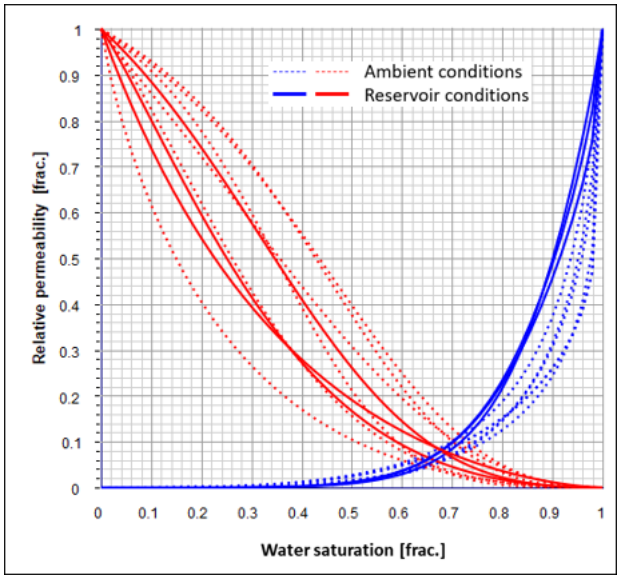

Fig. 17. Relative permeability, primary drainage, steady state, ambient vs. reservoir conditions, lin-lin plot.

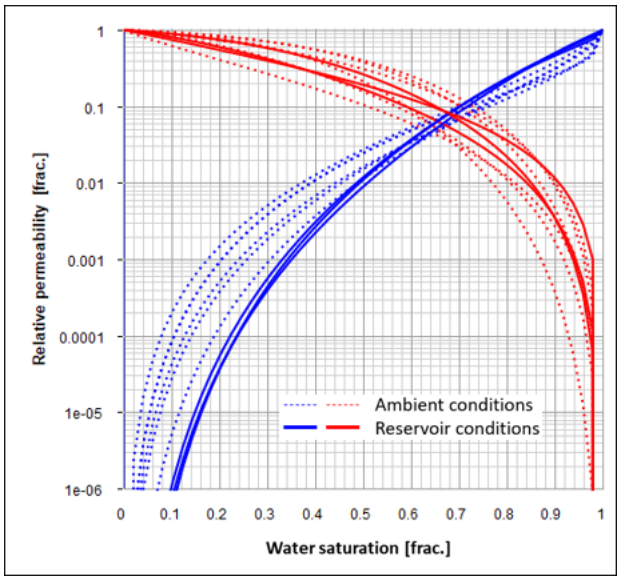

Fig. 18. Relative permeability, primary drainage, steady state, ambient vs. reservoir conditions, semilog plot.

For the lower water saturation region, all ambient conditions water relative permeabilities are above the reservoir conditions water relative permeabilities. However, uncertainty applies to the relative permeability curves in this region due to present limitations of the experimental equipment.

The combined steady state relative permeabilities are used as basis when defining the SCAL-model. The SCAL-model is shown by the grey curves in Fig. 19 and Fig. 20, base case together with the defined optimistic- and pessimistic case. When the relative permeability to CO_2 is low and the relative permeability to water is high, the SCAL-model is regarded as optimistic. The plume speed is hence lower, and the potential storage capacity is high as the water is more mobile than the base case. Like traditional SCAL-modelling of oil/water systems, if one

of the phases experiences low relative permeability the other phase experiences high relative permeability [15].

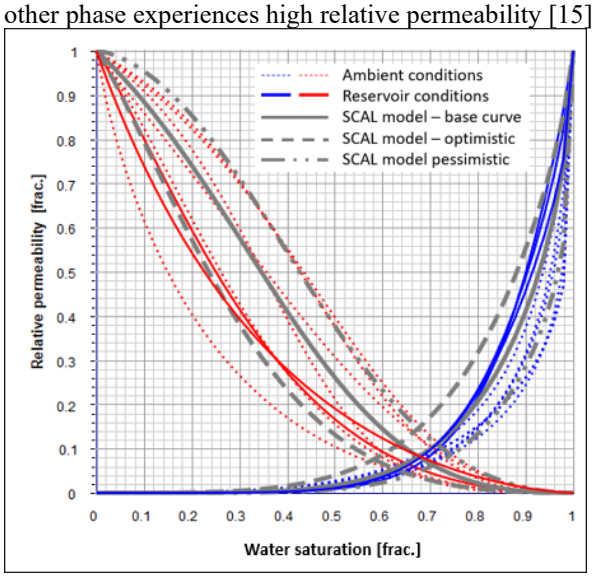

Fig. 19. Relative permeability for SCAL-model together with individual interpretation, lin-lin plot. Primary drainage.

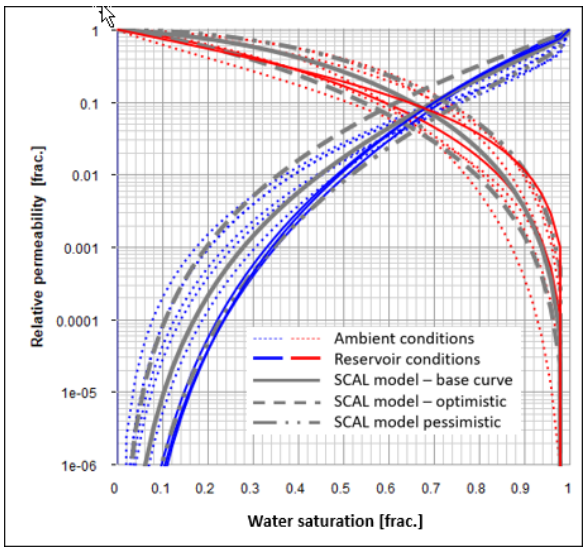

Fig. 20. Relative permeability for SCAL-model together with individual interpretation, semilog plot. Primary drainage.

The SCAL-model provides a huge variety of curves in the reservoir simulation model, acknowledging the uncertainty span both in the relative permeabilities and the residual water saturation vs. permeability trends as shown in Fig. 14 and Fig. 15.

As the plume speed and migration distance is the present focus for Northern Lights, the CO_2 relative permeabilities are defined in the pessimistic range. However, the water relative permeability honours the optimistic part to capture the ambient and reservoir condition curves in the entire saturation range, from unity to residual water saturation. Limited reservoir condition relative permeability experiments exist in the literature, but recent experiments at supercritical conditions indicates lower – and hence more optimistic CO_2 relative permeabilities toward residual water [13]. In this work it was decided to not be too optimistic to ensure robust decision making for Northern Lights.

The individual capillary pressure curves obtained by multi speed centrifuge and porous plate are shown in Fig. 21 while Fig. 22 shows the defined SCAL-model.

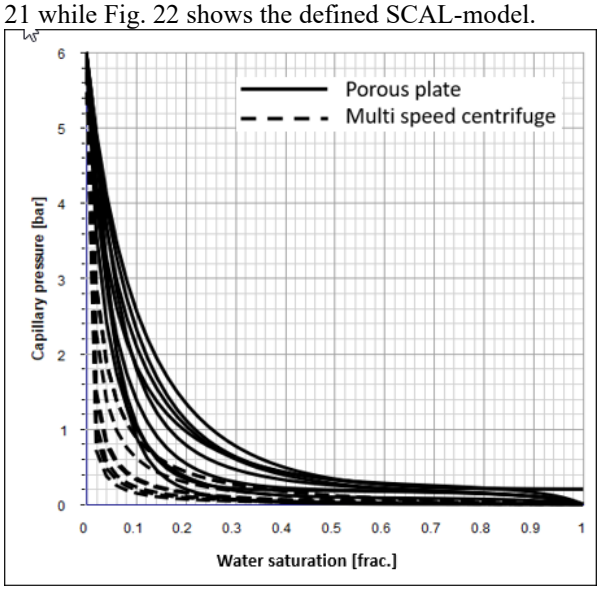

Fig. 21. Capillary pressure, porous plate and multi speed centrifuge, all ambient conditions. Primary drainage.

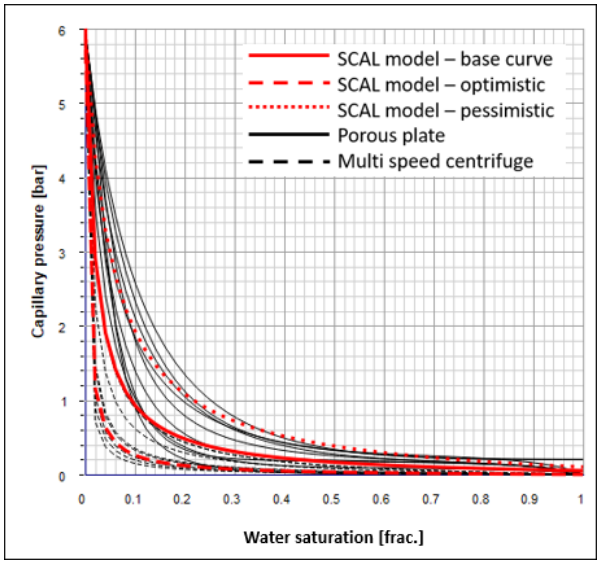

Fig. 22. Capillary pressure for SCAL-model that comprises all individual capillary pressure curves. Primary drainage.

As for the relative permeability curves, the capillary pressure is also scaled between zero and unity water saturation, in addition to be scaled to the maximum capillary pressure applied for the porous plate experiment as well as Leverett J-scaled with respect to different IFT for N_2/water and CO_2/water [14]. Even though the plugs used for multi speed centrifuge and porous plate are selected from the same area and are regarded as sister plugs, there is a remarkable difference between the capillary pressure determined from the multi speed centrifuge experiment and the porous plate experiments. When defining the capillary pressure for the SCAL-model, all experiments have been used without questioning the difference.

A base case capillary pressure curve has been established together with an optimistic and pessimistic span that comprises the uncertainty. For storage capacity

a low capillary pressure curve is regarded as optimistic due to less residual water saturation and hence larger capacity for CO_2. Consequently, a more pronounced capillary pressure curve will correspond to higher residual water saturation and less storage capacity for CO_2. The storage capacity will be an interplay between the buoyancy- and capillary forces and need further experiences from field applications. For plume migration, less capillary effects will increase the speed of the plume, and the optimistic and pessimistic curves can be argued to be switched. This is further discussed in section 5 and 6.

4.4 Imbibition, relative permeability and trapped CO_2

Trapped gaseous phase was obtained both at ambient condition utilizing N_2 and at reservoir conditions with CO_2. The semilog plot of the relative permeabilities obtained together with the base case of the SCAL-model subjected to uncertainty span utilizing a suggested optimistic and pessimistic curve is shown in Fig. 23. Contrary to trapped saturation for oil/gas systems, a high trapped saturation of CO_2 is regarded as optimistic for CCS – and low trapped CO_2 saturation is consequently pessimistic.

It was experienced that the water relative permeability at trapped N_2 for the individual ambient condition experiments where close to the individual water relative permeability curves for the primary drainage process as expected for strongly water-wet systems. However, even though the water relative permeability at trapped CO_2 at reservoir condition is still low, the end point water relative permeability experiences larger spread at reservoir conditions and did not necessarily follow the individual primary drainage water relative permeability curve. However, further implementation uses Killough [17] where input is residual water- and trapped gas saturation together with the primary drainage relative permeability curves used for the SCAL-model, see Fig. 19 and Fig. 20.

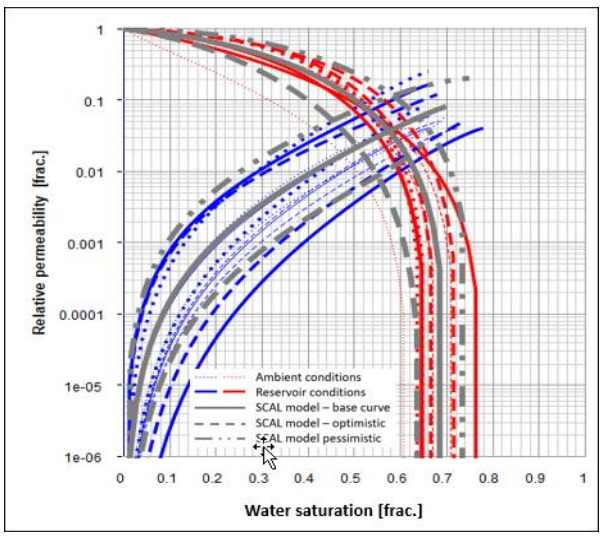

Fig. 23. Relative permeability for SCAL-model together with individual interpretation, semilog plot. Imbibition.

5 Field application: Results and observations

The SCAL model described in section 4 has been used for the Northern Lights dynamic simulation model. The simulation model uses Eclipse 300 with CO2STORE and relative permeability end point scaling options. The grid cell sizes are 200x200m in X-Y direction and between 1 to 7 m in average for the Z direction. The difference in cells thickness is partly a result of refinement of the grid in the Z direction below potential barriers to vertical flow, allowing for an acceptable handling of gravity segregation effect while keeping acceptable simulation times. The set-up assumes one injector injecting 1.5Mt CO_2 per year for 25 years. One of the purposes of the simulation model is to evaluate the risk of CO_2 to reach the northern license boundary and thus flow below the Troll Field before its end of production, assumed to be 2054. Sensitivities have been performed to evaluate the impact on CO_2 migration towards license boundary which is looked at in terms of maximum CO_2 distance reached from injection point versus time.

Simulation results provided in Fig. 24 show that the uncertainty of the relative permeability shape (Fig. 19 and Fig. 20) has an impact on the Maximum CO_2 distance reached at a given time.

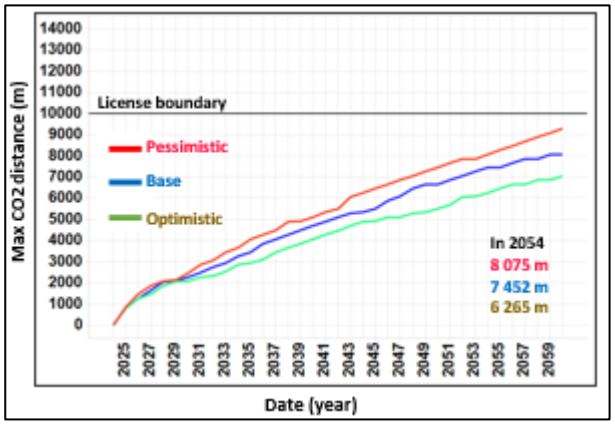

Fig. 24. Results from simulation of relative permeability shape uncertainty on maximum CO_2 migration distance.

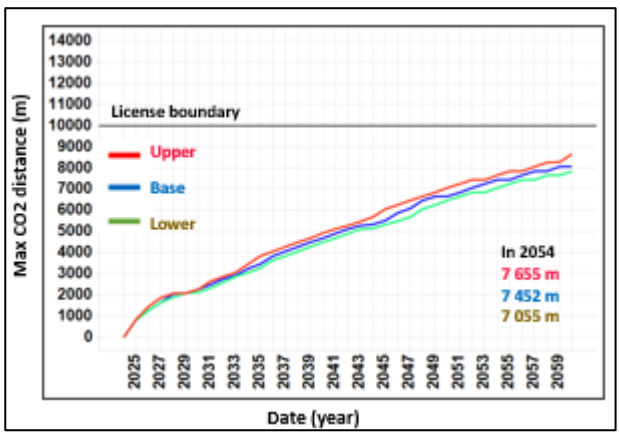

Fig. 25. Results from simulation of residual water saturation, S_{wr}, vs. permeability correlation uncertainty on maximum CO_2 migration distance.

Fig. 25, shows that the uncertainty of the correlation between residual water saturation, S_{wr} permeability has a lower impact than the relative permeability shape of the Maximum CO_2 distance reached at a given time.

The simulation results show that the uncertainty on the Land correlation [16] between trapped CO_2 and initial water saturation has no significant impact on the maximum CO_2 distance reached at a given time, see Fig. 26. However, the trapped CO_2 saturation has influence on the storage efficiency and especially after stop of injection when imbibition occurs.

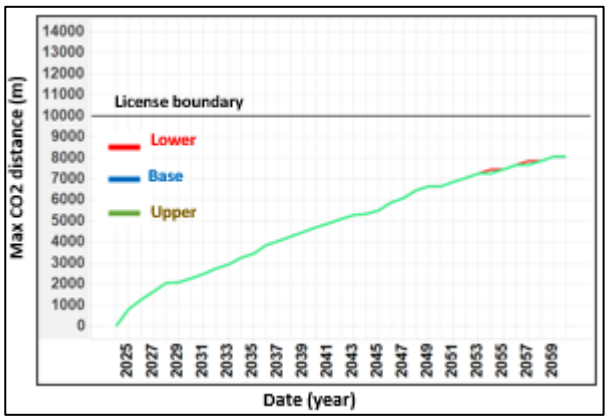

Fig. 26. Results from simulation of trapped CO_2 correlation to S_{wr} vs. k_w uncertainty on CO_2 migration distance versus time.

It was hence decided to not include the CO_2 trapped gas uncertainty on the ensemble-based model used to evaluate risk of CO_2 to cross the license boundary by 2054. The model ensembles allow for a consistent representation of uncertainty that propagates from the geological inputs to the simulated output.

The two other parameters - shape of relative permeability and S_{wr} vs. k_w correlation - have been accounted for in the ensemble-based model with the following probability distribution:

- Relative permeability shape:
  30% (pessimistic) - 40% (base) - 30% (optimistic)
- S_{wr} vs. permeability correlation:
  15% (pessimistic) - 70% (base) - 15% (optimistic)

The impact of the capillary pressure has also been evaluated using the base case relative permeability. As shown in Fig. 27, the CO_2 plume moves slightly further when zero capillary pressure is applied compared with including capillary pressure in the SCAL-model.

For a primary drainage process, this is as expected as a positive capillary pressure will act against the dynamic forces and reduce the speed of the CO_2 plume. The non-zero capillary pressure has been utilized in the simulation model.

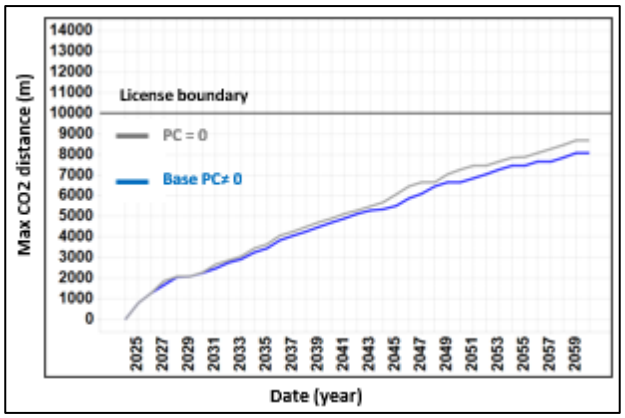

Fig. 27. Results from simulation of the capillary pressure effect on CO_2 migration distance versus time

6 Discussion

This study illustrates the importance of proper SCAL modelling for CCS based upon thorough SCAL-programs and interpretation. Even though the difference between ambient conditions and reservoir conditions may be argued to be limited, we encourage to proceed with experiments at reservoir- or supercritical conditions as the ambient conditions approach may lead to too pessimistic estimates of ultimate storage capacity. Further, it will be beneficial to modify the centrifuge- and porous plate techniques to enable reservoir conditions experiments and hence describe the fluid flow properties toward residual water saturation; shape of relative permeabilities, the end points - S_{wr}, $k_{rg}(S_{wr})$ - and the capillary pressure curve. By combining information from multiple experiments and various time dependent experimental data, the degree of freedom is limited, and a consistent SCAL-model can be constructed.

Multiphase flow of CO2 and water is presently at an immature state. The industry has generally limited experience with plume migration, ultimate storage capacity and long-term trapping mechanisms. From the core analysis point of view, several issues need to mature and some of them are discussed below.

Fingering effects. Primary drainage flow experiments are possibly influenced by fingering effects as the injected gaseous phase has significant lower viscosity than the displaced water. Utilizing steady state experiments are believed to minimize this effect compared to the unsteady state technique. Combining the centrifuge experiments with the steady state experiments, and observing the experimental response, especially the water saturation profiles, we argue that the experiments and interpretations are not significantly influenced by fingering effects.

Wettability. When injecting CO_2 into a virgin aquifer, the flow process will respond as a water-wet case, CO_2 being the non-wetting phase. It is not believed that the CO_2 will wet any parts of the minerals in pore-space due to lack of any surface-active compounds in addition that the water saturation will be relatively high in parts of the reservoir. Even though the CO_2 is not wetting the minerals, it may be reasonable to expect that the fluid flow process at pore level will be different for CO_2 and water than for N_2 and water at ambient conditions due to

different IFT, possible different spreading coefficients and other microscopic effects between the fluids and the appropriate minerals. If CO_2 is injected into depleted reservoirs the wettability may need to be addressed further as the mineral have seen oil and may not be strongly water-wet. Hence, the wettability of CO_2 and water of a pore surface possibly covered by hydrocarbon components may be affected.

Single speed centrifuge primary drainage experiments were done through the SCAL-program to gain information about the residual water and tail-end water relative permeability. However, these experiments provided unreliable high residual water saturation, S_{wr}, compared to the results from multi speed centrifuge- and porous plate experiments. This applied in the entire permeability range for all formations. All centrifuge experiments ensured a Bond no. less than 10^{-3} [2,3]. General experiences based upon Equinors internal SCAL-database is that the displaced phase tail-end relative permeability from single speed centrifuge experiments is frequently depressed compared to the appropriate property determined by steady state flow experiments. A consistent general explanation has not been established, and the single speed tail-end results have been omitted when establishing the SCAL-model. Proper interpretation of relative permeability at low water saturation is desired, and a deeper look into the physical behaviour of single-speed centrifuge experiments vs. multi-speed centrifuge- and flow experiments is encouraged.

Equilibrium between the phases. Experiments including supercritical CO_2 is very sensitive to the applied pore pressure and temperature, hence it is crucial to establish very good control of these parameters. Equilibrium between the phases is required for any relative permeability experiment, and state of the art multi-phase flow apparatuses ensures this. However, temperature can be a challenge as the core holder is placed in another specially designed heating cabinet to enable monitoring of ISSM. Necessarily, there are tubes from the pumps and fluid cells to the core holder, and these need to be kept at system temperature. If there is a temperature difference between these parts of the flow apparatus, it may affect the equilibrium and hence the saturation in the composite core. In the present set-up there was a challenge to keep the temperature stable, however it is solved by high performance heated pipes surrounding the flow tubes between the heating cabinet and the core holder. [19].

Interpretation and core flow simulations. Throughout this work all experiments have been history matched by Sendra [4], utilizing the flexible, but smooth LET correlations for relative permeability [6] and capillary pressure [7]. The purpose is to gain information from different type of experiments, and hence fluid flow information and end points along the entire saturation range [5]. The interpretation is done sequentially by first history matching production data for the multi speed centrifuge experiment by simulation, then secondly history match the steady state experiment. As only one type of experimental data – production data – is history matched, multi-speed experiments can be regarded as an ill-posed problem with multiple solution if capillary pressure, relative permeability and the end points are not subjected to proper constraints. We utilize the history match by anchoring the flow properties, i.e. k_r and P_c in the obtained residual water saturation as a first estimate. Then the first estimate of flow properties is the curve fitted LET of the analytical capillary pressure from the multi speed centrifuge experiment and the LET curve fitted analytical relative permeability data from the steady state experiment. The history match is done by adjusting the shape and possible threshold pressure of the capillary pressure curve only. After this, if necessary, the saturation end point, S_{wr}, is adjusted and finally – if necessary, the shape of the tail-end water relative permeability is adjusted. When the capillary pressure curve and S_{wr} are concluded, these properties act as input when history matching the steady state experiment by varying the shape of the relative permeability curves. The relative permeability curves from steady state are then sequentially used in the appropriate multi speed centrifuge simulation to enable any required tuning of the initially used relative permeability curves. This is done throughout the interpretation of all experiments in the SCAL program.

Super critical conditions. Capillary pressure will probably influence the ultimate storage capacity and efforts should be done to determine capillary pressure at reservoir conditions or applying a variety of supercritical conditions.

SCAL model uncertainty. Throughout this work we have used the terms base-case curves subjected to uncertainty by applying a set of optimistic- and pessimistic curves. The terms are well established for oil- and gas exploration, but not for CCS. What is regarded as optimistic with respect to ultimate storage may not be optimistic for plume migration and speed. Low capillary pressure is regarded as optimistic for ultimate storage capacity but is regarded as pessimistic for plume migration and speed. However, high amount of trapped CO_2 will obviously be optimistic for CCS. Utilizing the applied correlations, S_{wr} vs. k_w and Land for trapped CO_2 may also open for discussions of these terms – when related to plume migration and ultimate storage.

7 Conclusions and recommendations

In this study the following conclusions and recommendations are drawn:

- Shape of the relative permeability curves impact the plume migration and ultimate storage – uncertainty span must be included.
- Residual water saturation influences the plume migration and ultimate storage and should be correlated with permeability – uncertainty span is recommended but can be omitted.
- Trapped gas vs. initial saturation does not influence plume migration speed but affects ultimate storage. Uncertainty not required to estimate plume speed- and migration.

- Capillary pressure influences plume speed- and migration. Zero capillary pressure is the most pessimistic and capillary pressure can be omitted when plume speed and distance is studied.
- Capillary pressure and trapped gas correlations should be included for ultimate storage capacity.
- Imbibition water relative permeability followed the primary drainage curve at ambient conditions with N_2, but not necessarily at reservoir conditions with $scCO_2$.
- Utilize end point scaling and utilize the SCAL-model scaled by the correlation of residual water saturation vs. permeability.
- We encourage to get more data at supercritical conditions toward low water saturations.
- Acknowledge that more insight into fluid flow parameters at supercritical conditions are required, both at plug scale and at reservoir scale.

Acknowledgement

Northern Lights JV DA and Equinor ASA are acknowledged for giving permission to publish the data. Especially thanks to Else Birkeland Johannesen (Equinor ASA) for valuable discussions and comments to the manuscript – highly appreciated.

References

1. Meneguolo, R., Sundal, A., Martinius, A. W., Veselovsky, Z., Cullum, A., and Milovanova, E. (2022) Impact of the Lower Jurassic Dunlin Group depositional elements on the Aurora CO_2 storage, EL001, Northern North Sea, Norway. *International Journal of Greenhouse Gas Control*, **119**, 103723. DOI: 10.1016/j.ijggc.2022.103723.
2. PcPhee C., Reed, J. and Zubizarreta, I.: «Core Analysis: A Best Practice Guide», Developments in Petroleum Science, Volume 64, Elsevier, 2015.
3. Hirasaki, G. J., Rohan, J.A. and Dudley, J.W.: «Interpretation of Oil-Water relative Permeabilities from Centrifuge Experiments», SPE Advanced Technology Series, Vol. 3, No. 1, pp. 66-75,1995.
4. Sendra User guide 2020.1, PRORES AS, 2020.
5. Sylte, A., Ebeltoft, E. and Petersen, E.B.: «Simultaneous Determination of Relative Permeability and Capillary Pressure Using Data from Several Experiments». Paper SCA 2004-08 presented at the International Symposium of the Society of Core Analysts, Abu Dhabi, UAE, 5-9 October 2004.
6. Lomeland, F., Ebeltoft, E., and Thomas, W.H.: «A New Versatile Relative Permeability Correlation». Paper SCA 2005-32 presented at the International Symposium of the Society of Core Analysts, Toronto, Canada, 21-25 August 2005.
7. Lomeland, F., and Ebeltoft, E.: «A New Versatile Capillary Pressure Correlation». Paper SCA 2008-08 presented at the International Symposium of the Society of Core Analysts, Abu Dhabi, UAE, 29 October – 2 November 2008.
8. Forbes P.L., 1991: «Simple and accurate methods for converting centrifuge data into drainage and imbibition capillary pressure curves». 1991 Society of core analysts annual technical conference, August 20-22, San Antonio, paper 9107, 15p.
9. Forbes P.L., 1993: «Centrifuge determination of Capillary Pressure - Review of data analysis procedures». Workshop. SCA - 7th Annual Technical Conference of the Society of Core Analysts, Houston, Aug. 9-11, 1993, Proceedings.
10. Hagoort, J.: «Oil Recovery by Gravity Drainage» SPEJ (June 1980), 139-150.
11. Nordtvedt, J.E. and Kolltveit, K., «Capillary Pressure Curve from Centrifuge Data by Use of Spline Functions,» SPE Unsolicited paper 19019.
12. R. L. Boyer, F. Morgan, and M. Muskat: «A New Method for Measurement of Oil Saturation in Cores» Trans. AIME, 170, 15 (1947).
13. Mascle, M., Oisel, A., Munkerud, P.K., Ebeltoft, E., Lopez, O., Pryme, C., Youssef, S.: «CO_2-Brine Relative Permeability Measurements at Reservoir Conditions: how to reconciliate SS and USS methods». To be presented at the International Symposium of the Society of Core Analysts, Abu Dhabi, UAE, October 9-12, 2023.
14. C.A. Aggelopoulos, C.A., Robin, M., Vizika, O.: «Interfacial tension between CO2 and brine (NaCl + CaCl2) at elevated pressures and temperatures: The additive effect of different salts», Advances in Water Resources 34 (2011) 505–511.
15. Ebeltoft, E., Lomeland, F., Brautast, A., Haugen, Å.: «Parameter Based SCAL - Analysing Relative Permeability for Full Field Application», reviewed Proceedings of the 2014 International Symposium of the SCA, Avignon, France, September 8-11, 2014.
16. Land, C.S. 1971. «Comparison of Calculated with Experimental Imbibition Relative Permeability», SPE J. 11 (4): 419–425. SPE-3360-PA.
17. Killough, J. E. «Reservoir Simulation with History-dependent Saturation Functions», paper SPE 5106, Society of Petroleum Engineers Journal (1976) 16, No. 1, 37-48.
18. Swanson, B.F. 1981. «A Simple Correlation Between Permeabilities and Mercury Capillary Pressures.» J Pet Technol 33 (12): 2498-2504. SPE-8234-PA. http://dx.doi.org/10.2118/8234-PA.
19. RS Systems AS, Fosnavaag, Norway. www.rs-systems.no